Shunsuke Terasaka, M.D., J. Diaz Day, M.D., and
Takanori Fukushima, M.D., D.M.Sc.

Extended Transbasal Approach: Anatomy, Technique, and Indications

ABSTRACT—Appropriate indications for the transbasal approach have not been clearly established. The focus of this study is to determine the feasibility of maximal exposure of the clivus and surrounding regions via this strategy. Further, we sought to determine the key anatomical landmarks and morphometric data necessary for safe, radical exposure. In 20 injected cadaveric specimens, anatomical observations were made grossly and microscopically with 4–40× magnification. The three basic variations of the transbasal craniotomy were compared with regard to surgical exposure. Maximum exposure of the ventral clivus could be obtained by total ethmoidectomy and sphenoidectomy through the extensive transbasal craniotomy. The lateral limits of exposure were found to be the optic nerves, intracavernous carotid arteries, and hypoglossal canals. Inferiorly, the foramen magnum is the limit of exposure. Morphometric measurements were determined between the key landmarks and were found helpful in subsequent dissections due to the lack of bony structures in relation to neural and vascular structures within the bone. The keys to optimizing the transbasal approach are beyond the simple initial steps of the craniotomy. Maximal exposure from the suprasellar compartment to the foramen magnum is possible via the extended transbasal approach.

In 1913, Frazier[1] outlined his early concept of the bifrontal craniotomy, which formed the basis for the transbasal approach. Tessier and Derome[2,3] were the first to develop a systematic transbasal technique for craniofacial reconstruction and anterior skull base lesions. Recent advances in technique and instrumentation have resulted in expansion of the basic technique and application to not only anterior skull base lesions, but those involving the middle and posterior fossa as well.[4] Numerous modifications have been used to refine the approach.[4–11] Kawakami described an en bloc bilateral osteotomy of the orbital roofs and frontal sinus as a term "extensive transbasal approach" in 1991. Sekhar[4] presented some variations for orbitofrontoethmoidal osteotomy depending on the tumor location as a term "extended frontal approach" in 1992. He also revealed excellent clinical results via this approach. Raveh[10] described advanced frontonasoorbital osteotomy including the lacrimal crest as a "extended anterior subcranial approach" in 1995. These modifications have mainly differed in the location of the naso-orbital osteotomy and reconstruction of the anterior skull base. The focus of previous communications has been on the initial cranial opening. However, little attention has been paid to the precise differences in exposure that these alternative methods provide. Further, the suggested indications for each modification have been relatively broad. It is diffi-

Skull Base Surgery, Volume 9, Number 3, 1999. Allegheny University of the Health Sciences, Center for Skull Base Surgery, Pittsburgh, Pennsylvania. Reprint requests: Dr. Terasaka, Department of Neurosurgery, Hokkaido University, Kita-ku, North 15 West 7, Sapporo 060, Japan. 1052–1453/1999/E1098–9072(1999)09:03:0177–0184:SBS00142X

cult to glean from the literature what are the proper indications for each particular technique.

The extended transbasal approach is defined as a bifrontal craniotomy combined with removal of the supraorbital bar, ethmoidectomy, sphenoidectomy, and extradural resection of the clivus. In this study, the precise anatomical landmarks and limits of exposure of the extended transbasal approach were delimited. We studied the critical steps of the approach beyond the initial cranial opening, which are crucial to maximal exposure.

MATERIALS AND METHODS

Twenty adult cadaveric specimens, the vessels injected with colored silicone, were utilized for the study. Dissections were performed grossly and under magnification with a surgical microscope. Morphometric measurement were made with small calipers and metric scale. The surgical technique of the extended transbasal approach was broken down into five major components: (1) scalp reflection and craniotomy, (2) ethmoidectomy and sphenoidectomy, (3) orbital apex and cavernous sinus dissection, (4) clivectomy, and (5) intradural dissection. The critical anatomical structures, that is, those constituting major surgical landmarks, relevant to the optic nerve, carotid artery, vidian nerve, and hypoglossal canal were observed and morphometric measures taken. All observations and measurements were made from the surgeon's angle of view.

Surgical Approach

Step 1: Scalp Reflection and Craniotomy

A bicoronal scalp incision was made beginning from the preauricular crease bilaterally. The scalp was ele-

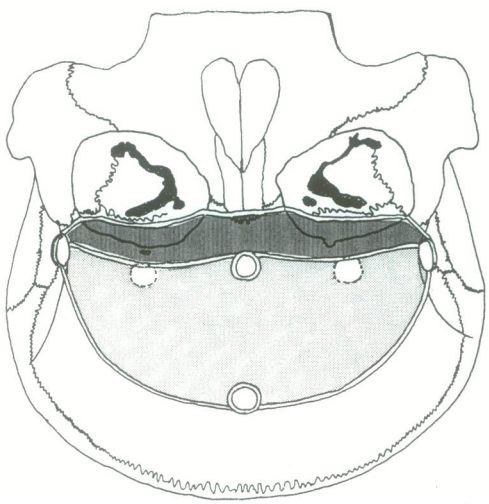

A

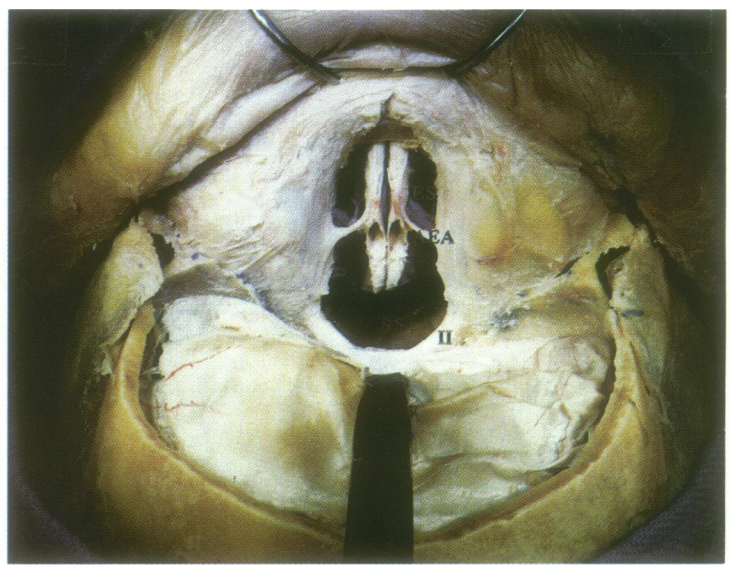

B

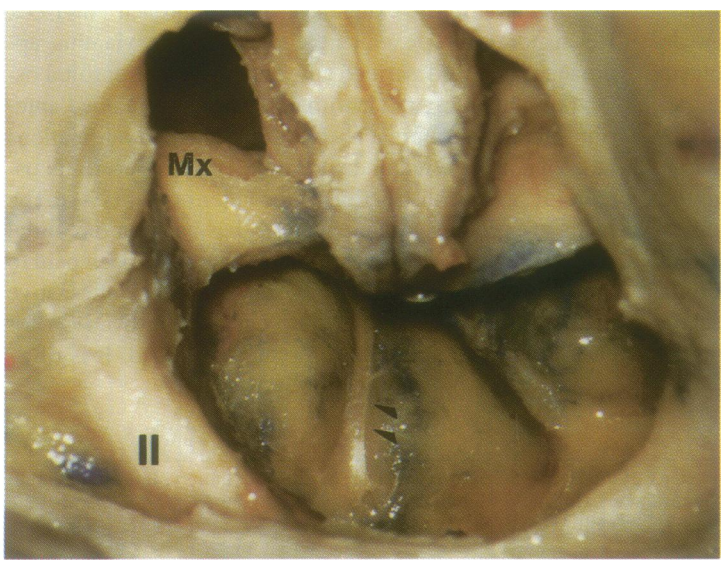

C

Figure 1. (A) Schematic drawing showing the bifrontal craniotomy (light shadow) and supraorbital bar (dark shadow). Four burr holes are usually necessary for the bifrontal craniotomy and two additional holes are required in some cases. The nasofrontal and frontozygomatic sutures are marker for the osteotomy of the supraorbital bar. (B) The honey-comb-like ethmoid air cells were removed with rongeurs to expose the midline nasal septum. The sphenoid sinus was then opened completely. The corridor into the sphenoid sinus through removal of the planum sphenoidale was found to be roughly trapezoidal in shape. Nasal mucosa is keep intact with anterior ethmoidal arteries. II = optic nerve; AEA = anterior ethmoidal artery; ES = ethmoid sinus; and SS = sphenoid sinus. (C) The vidian canal (arrow head) is observed in the inferolateral wall of the sphenoid sinus in 44% of specimens. II = optic nerve; and Mx = Maxillary sinus.

vated, preserving vascularized pericranium medial to the linea temporalis of each side. Over the temporalis muscles, the superficial temporal fat pads were elevated with the scalp flap to protect the frontalis branches of the facial nerve. The pericranium and scalp flap were elevated to expose the supraorbital rim and glabella. Medial, the inferior limit of exposure was nasofrontal suture. The supraorbital and supratrochlear nerves were released from their foramina, if present, by bone removal. Periorbital fascia was next elevated away from the superior and lateral walls of the orbit. The temporalis muscle and fascia were elevated at their anterior superior attachment to expose the region of the sphenofrontal suture and pterion.

Four burr holes were made and bifrontal craniotomy was performed (Fig. 1A). The initial two holes were made at the orbitotemporal region and the other two holes were at the midline. In some cases, additional two holes are necessary at just above the supraorbital foramen (Fig. 1A). After removing the bone flap, the subfrontal dura was elevated. The supraorbital bar was then removed with an oscillating saw and with small osteotomes (Fig. 1A). The medial inferior osteotomy was made at the nasofrontal suture. Laterally, the frontozygomatic suture was used as the marker for the osteotomy. The osteotomy through the orbital roof was performed in such a way as to preserve the attachment of the medial canthal ligament.

After removal of the supraorbital bar, the posterior wall of the frontal sinus was removed with the high-speed drill. The sinus was exenterated of all mucosa and the ostia identified. The dural sleeves attaching around the cribriform plate area were incised, thus interrupting the olfactory bulbs. The dural sleeves were then closed in water-tight fashion.

Step 2: Ethmoidectomy and Sphenoidectomy

The high-speed drill was next used to open the cribriform plate area and planum sphenoidale to expose the ethmoid and sphenoid sinuses. The honey-comb like ethmoid air cell were removed with rongeurs to expose the midline nasal septum. The sphenoid sinus was opened completely, removing any sphenoid septae that were present.

Step 3: Orbital Apex and Cavernous Sinus Dissection

The optic canals were skeletonized by drilling at the posterior lateral aspect of the sphenoid sinus opening. The lateral wall of the sphenoid sinus and medial wall of the cavernous sinus were then removed to expose the carotid artery through its intracavernous course. The anteromedial cavernous sinus was then dissected after bone removal.

Step 4: Clivectomy

The drill was then used to remove the clival bone, until exposing the clival dura. Dissection of the lower clivus extended laterally. This procedure continued until exposing the hypoglossal canals bilaterally.

Step 5: Intradural Dissection

As a final step, the clival dura was opened in the midline and retracted lateral. The subfrontal dura was also opened across the tuberculum sellae region. Observations were then made microscopically.

RESULTS OF DISSECTION AND MORPHOMETRIC ANALYSIS

Step 1: Scalp Reflection and Craniotomy

With regard to scalp reflection, we found that adequate exposure to the level of the nasofrontal suture may be difficult in some cases. In this regard, we found the technique described by Fujitsu et al[12] to be helpful. This technique involves midline incision of the procerus muscle, which relaxes the scalp and leads to easier exposure of the nasion. We also found the disruption of the attachments of the medial canthal ligaments was unnecessary for adequate exposure and has obvious postoperative cosmetic benefits.

Removal of the supraorbital bar was found to be most effective with the lateral landmark for osteotomy being the frontozygomatic suture. The inferomedial landmark was nasofrontal suture. It was easier to remove this section of bone after first interrupting the olfactory bulbs at the cribriform plate and removing the crista galli. Alternatively, we found the method of Spetzler et al[11] to preserve the olfactory nerves and mucosa to be feasible. Anatomically, one has to bear in mind the location of the anterior superior ethmoidal and posterior superior ethmoidal arteries and ligate them proximal to their dural anastomoses.

Step 2: Ethmoidectomy and Sphenoidectomy

The honey-comb like structure of the ethmoid sinus results in difficulty distinguishing nasal mucosa from the thin septae of the sinus. This is especially true regarding the anterior half of the sinus. Here, removal of the air cells inevitably results in entering the nasal cavity through the superior or middle meatus. The nasal mucosa is more distinguishable from the perpendicular plate of the ethmoid. Following posterior and inferior, separating the mucosal layers in the midline, exposes the vomer and the sphenoid rostrum.

We found the course of the optic nerves to be unpredictable by the superficial appearance of the planum sphenoidale. Important in locating the terminal end of the optic canal was complete dural elevation to lesser

wing of the sphenoid and over the anterior margin of the tuberculum sellae. The corridor into the sphenoid sinus through removal of the planum sphenoidale was found to be roughly trapezoidal in shape (Fig. 1B). Measurements of this trapezoidal corridor were taken and are summarized in Table 1. The width of the trapezoid at its anterior base (defined by line connecting the tendinous rings) averaged 30 ± 3.3 mm (range = 25 to 36 mm). The posterior base (defined by the line connecting the terminae of the optic canals) averaged 13 ± 2.9 mm (range = 8 to 19) in width. The height of this corridor averaged 14.5 ± 4.0 mm (range = 9 to 23).

The sphenoid sinus was rarely equally divided in volume by a bony septum. Several bony prominences were observed on the lateral wall of the sinus in sellar and presellar types. The carotid prominence was found in 72%. A prominent optic canal was observed more frequently, being easily distinguished bilaterally in 94% of dissections. In the inferolateral aspect of the sinus, the maxillary division of the trigeminal nerve protruded into the sinus in 39%. Compared with previous studies, these percentages are somewhat less.[13,14] Additionally, the vidian canal could be distinguished in the inferolateral wall in 44% of specimens and is demonstrated in figure 1C.

Step 3: Orbital Apex and Cavernous Sinus Dissection

Particular attention was paid to the carotid artery in this portion of the dissections. The cavernous carotid artery (CCA) was the most medial structure within the cavernous sinus and its size and course varied. From the surgeon's view, the posterior vertical portions (C5 segment) of the arteries came closest together, essentially defining the lateral limits of exposure at this level of the dissection. The distance between the segments averaged 17.6 ± 3.4 mm (range = 13 to 24 mm). At the level of the foramen lacerum, the artery is bordered inferiorly by a thick fibrobasilar cartilage. The interarterial distance at this point (C5–C6 segment junction) averaged 22.9 ± 2.8 mm (range = 19 to 31 mm) (Figs. 2A and 2A'). In most cases, a carotid prominence was not visible where the artery entered the foramen lacerum. The most helpful landmark in this respect is the pharyngobasilar fascia, which may be traced laterally to find the position of the carotid at the foramen lacerum (Fig. 2B). Removal of several millimeters of clival bone was necessary to locate the carotid artery at this level. The width between the carotid arteries at the anterior bend of the vessel averaged 22.1 ± 2.2 mm (range = 19 to 25 mm). This junction measured 59.8 ± 4.3 mm (range = 53 to 70 mm) deep in the operative field, measured from the nasion.

To expose the neural elements around the orbital apex, the optic canal has to be fully drilled out at first. The base of the anterior clinoid process (lateral optic strut) is also removed to mobilize the optic nerve laterally. The neural structures at the orbital apex and the cavernous sinus were observed (Figs. 2C and 2C'). The oculomotor nerve appears inferior to the ophthalmic artery, where it divides into its inferior and superior rami before passing through the annular tendon. The trochlear nerve and the frontal branch of V1 are crossing over the oculomotor nerve in this area. The entire course of the abducens nerve was not easily visible via this exposure unless the CCA was displaced laterally (Fig. 2D). For pursuing a further dissection toward to the intraconal space, the annular tendon that is packed with critical neurovascular structures should be opened.

The vidian nerve, composed of the greater superficial petrosal and deep petrosal nerves, was observed in the inferolateral portion of the surgical field. In 44% of specimens, the bony prominence covering the nerve was visible. Carefully drilling technique is required to

Table 1. Anatomical Measurements in 20 Cadaveric Specimens

Site of measurements	*Average ± SD (mm)*	*Range (mm)*
Trapezoidal corridor		
anterior base	30.0 ± 3.3	25 – 36
posterior base	13.2 ± 2.9	8 – 19
height	14.5 ± 4.0	9 – 23
Distance between		
C3–C4 junctions	22.1 ± 1.8	19 – 25
C5 segments	17.6 ± 3.4	13 – 24
C5–C6 junctions	22.9 ± 2.8	19 – 31
vidian canals	29.3 ± 3.2	23 – 34
hypoglossal canals	25.8 ± 2.2	22 – 31
Depth of		
C3–C4 junction*	59.8 ± 4.3	53 – 70
hypoglossal canal**	41.1 ± 4.0	31 – 48
Distance from sella to pharyngobasilar fascia	19.9 ± 40	13 – 26

*from Nasion
**from pituitary gland

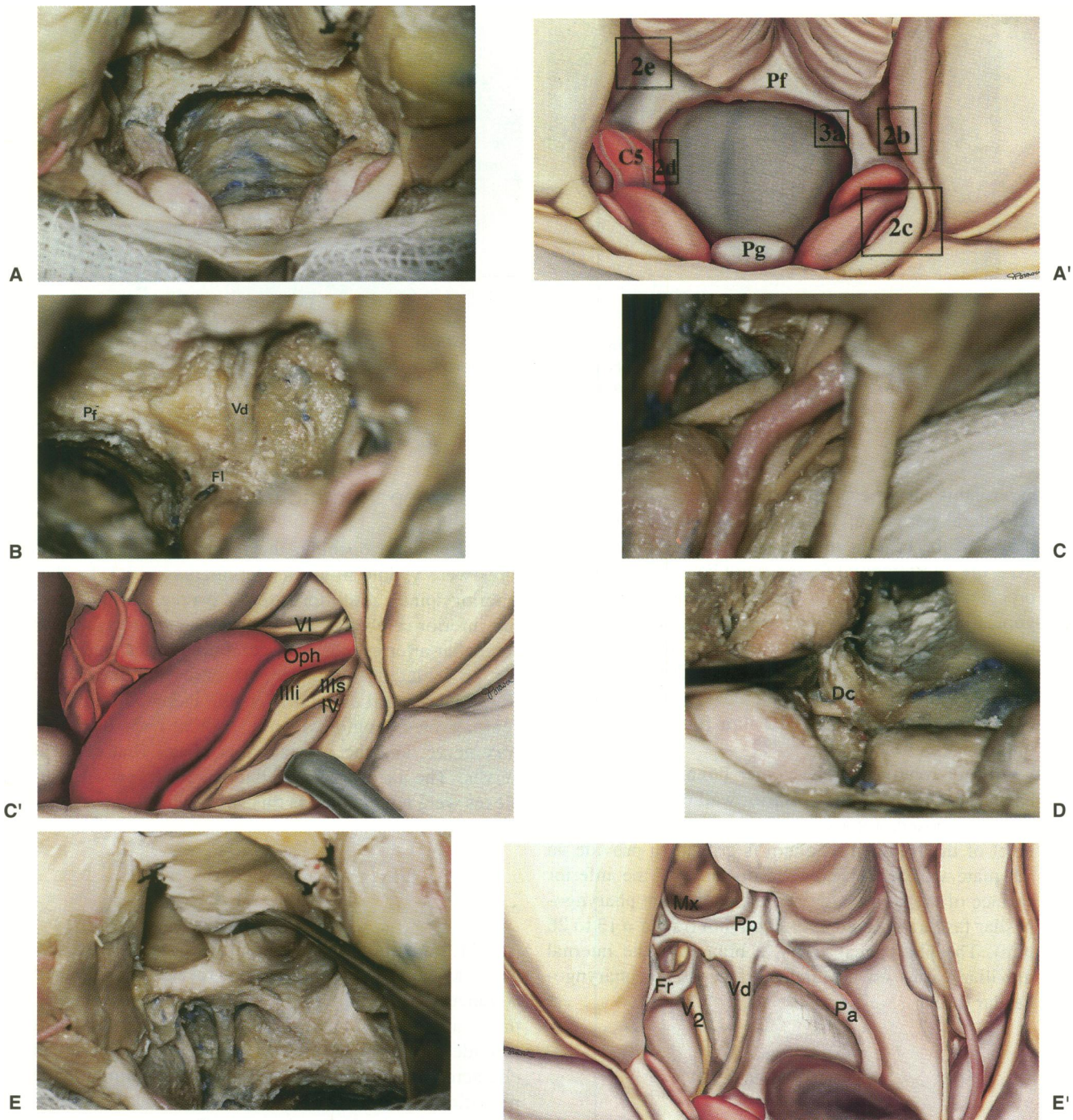

Figure 2. (A) The posterior vertical portions (C5 segments) of the cavernous carotid arteries come close together whose sizes and courses varied. At the level of the foramen lacerum, the artery is bordered inferiorly. (A') Scheme of Figure 2A. Each rectangle box shows where each of the following magnified photographs were taken. C5 = C5 segments; Pf = pharyngobasilar fascia; and Pg = pituitary gland. (B) Anatomical structures around the right foramen lacerum. The vidian nerve is shown in the center of photograph. Fl = foramen lacerum; Pf = pharyngobasilar fascia; and Vd = vidian nerve. (C) The neural structures at the right orbital apex are shown. It is noted that the oculomotor nerve appears inferior to the ophthalmic artery, where it divided into its inferior and superior rami. The medial part of the annular tendon is incised to expose the oculomotor and abducens nerves. (C') Scheme represents anatomical relationship of the cranial nerves at the orbital apex and the carotid artery in the cavernous sinus. IIIs = superior rami of the oculomotor nerve; IIIi = inferior rami of the oculomotor nerve; IV = trochlear nerve; VI = abducens nerve; and Oph = ophthalmic artery. (D) Left Dorello's canal is exposed with lateral displacement of the cavernous carotid artery. Dc = Dorello's canal. (E) Anatomical structures around the left pterygopalatine ganglion. The pharyngeal artery runs on the undersurface of the pharyngobasilar fascia. The maxillary sinus is opened. (E') Scheme of Figure 2G. V2 = maxillary nerve; Fr = foramen rotundum; Mx = maxillary sinus; Pa = pharyngeal artery; Pp = pterygopalatine ganglion; and Vd = vidian nerve.

Figure 3. (A) Right hypoglossal canal is shown. The hypoglossal canals form the lateral limits of exposure at this level. Hc = hypoglossal canal. (B) Intradural observation via this approach. XII = hypoglossal nerve; Ba = basilar artery; AICA = anterior inferior cerebellar artery; Va = vertebral artery.

expose this nerve because of its fragility. Drilling the inferolateral portion of the sphenoid sinus results in removal of the base of the lateral pterygoid plate. However, the infratemporal fossa cannot be accessed via this procedure. This nerve is exposed between the pterygopalatine ganglion and the foramen lacerum where it is hardly distinguishable from the surrounding thick fibrous tissue (Figs. 2E and 2E'). The width of the interval between the two sides at its most proximal point of exposure averaged 29.3 ± 3.2 mm (range = 23 to 34 mm).

After removal of the vomer bone, the pharyngobasilar fascia, lining the posterior wall of the hypopharynx is exposed. Exposure of this fascia down to the level of the foramen magnum is critical to provide an adequate working space. The distance of the inferior surface of the sella to the nearest part of the pharyngobasilar fascia averaged 19.9 ± 4.0 mm (range = 13 to 26 mm). The pharyngeal artery, a branch of the internal maxillary, runs on the undersurface of the pharyngobasilar fascia.

Step 4: Clivectomy

Removal of the clivus provided access as inferior as the foramen magnum. Laterally, the limits of removal were found to be the hypoglossal canals in the condylar portion of the occipital bone (Fig. 3A). The width between the hypoglossal canals averaged 25.8 ± 2.2 mm (range = 22 to 31 mm). The depth of the hypoglossal canals, measured from the pituitary gland to a line connecting the canals of two sides, averaged 41.1 ± 4.0 mm (range = 31 to 48 mm). Superiorly, the posterior clinoid processes were located in a sort of " dead angle", out of view. This portion of bone of the sella could be exposed and removed if the pituitary gland was mobilized out of its fossa, moving it superior.

Step 5: Intradural Dissection

After dural opening, the following arterial structures were visible in all dissections; vertebral, basilar, anterior spinal, posterior inferior cerebellar, and anterior inferior cerebellar. In some specimens, the superior cerebellar arteries, posterior cerebral arteries, and basilar top including thalamic perforators could be seen (Fig. 3B). Neural structures visible included the abducent nerves, hypoglossal nerves, spinal roots of accessory nerve, and the ventral roots of the first cervical nerves. The facial and vestibulocochlear nerve complexes were not visible via this approach.

DISCUSSION

Minimization of complications in skull base surgery has benefited greatly by our recent technological advances. Despite certain of these improvements, these approaches have inherent characteristics that provide for surgical pitfalls based upon anatomical characteristics. The transbasal approach maintains the potential for vascular, neural, and infectious complications.[15] To reduce the chances of such problems, a thorough understanding of the precise microsurgical anatomy of this approach should be helpful. Further, the variations that exist of the basic transbasal approach demand some selection criteria for their utilization. Although many previous reports have presented surgical modifications for naso-orbital osteotomy and reconstruction, most have lacked a description of the surgical anatomy encountered after sphenoidectomy. Based upon our detailed anatomical work, several surgical pitfalls were identified. Also, criteria for approach selection based upon the specific anatomical structures involved were developed.

Anatomical Considerations

The transbasal approach provides exposure from the third ventricle to the base of the clivus, generally with limited frontal lobe retraction. The degree of retraction depends in large part upon the initial craniotomy utilized, whether it involve osteotomy of all or part of the supraorbital bar. However, as can be inferred from the results of this study, the keys to optimizing exposure are beyond the simple initial steps of the craniotomy.

Lateral exposure in the clival region is limited largely by the position of the intracavernous carotid artery. The morphometric data may be some help to gauge the working area to the midclival region. Clinically, the preoperative magnetic resonance imaging (MRI) study is used to determine this area in the individual patient. Coronal cuts through the cavernous sinus provide these data. During surgery, the relationship of the pharyngobasilar fascia to the location of C5 portion of the vessel should be kept in mind. This fascial band is traced lateral and posterior to locate the vessel in the region of the foramen lacerum. Tracing the vidian nerve, which merges with the lateral surface of the C5–C6 junction is also helpful to predict the exact location of the vessel during removal of the upper clivus. Some of our morphometric values showed a discrepancy from previous reports. The difference is most likely secondary to the surgical orientation we used to take the measurements, in contrast to those in strictly anatomical preparations.

We found the inferior limit of exposure to be the foramen magnum. In this region, the hypoglossal canals may also be exposed, which has not been described before in utilizing this approach. The hypoglossal canals form the lateral limits of exposure in the inferior extent of the exposure, akin to the carotid arteries more superior. However, the hypoglossal canals do not enjoy an easily identifiable landmark that signals their location. Therefore, the morphometric information provided here is helpful in this regard.

Approach Selection

Controversy still exists regarding the indications for the various modifications of the transbasal approach. Based upon our cadaver dissections, we have come to several conclusions. The standard transbasal approach can provide an adequate exposure of the nasal cavity and the paranasal sinuses. However, dissection of the clivus requires a moderate degree of frontal lobe retraction for an adequate working space (Fig. 4). Frontal lobe damage may occur secondary to excessive retractor pressure. Partial removal of the supraorbital bar, medial to the supraorbital notches, has advantages in dissection toward the clivus as compared to the standard transbasal approach. The added midline removal of bone allows for resection of the upper and middle clivus without significant frontal lobe retraction. However, this is a laterally restricted approach. Therefore, the medial aspect of the cavernous sinus and lateral structures such as the hypoglossal canals are more difficult to expose. The extended transbasal approach is defined by complete removal of the supraorbital bar. The real advantage to this modification in the craniotomy is the ability to expose the lateral structures. The supraorbital bar does not provide an obstruction in this case to looking in the inferior and lateral compartments.

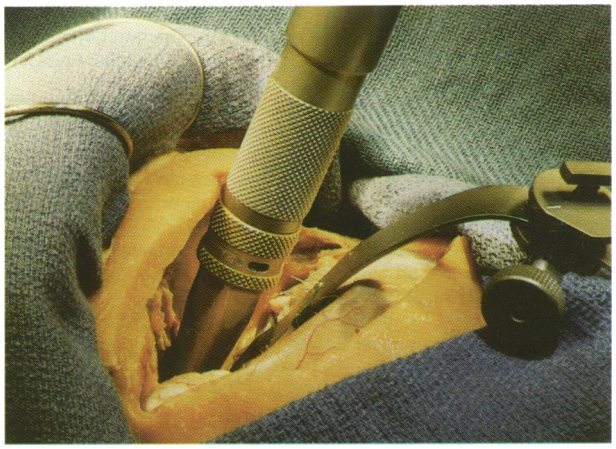

Figure 4. The supraorbital bar impedes clival drilling without excessive frontal retraction.

Based upon our observations in the laboratory, we have developed criteria for approach selection. For lesions confined to the frontal fossa and paranasal sinuses, the standard transbasal approach is indicated. When the lesion extends to the upper and/or middle clivus, without cavernous sinus extension, the standard transbasal approach with partial removal of the supraorbital bar is chosen. In any case with extension of the lesion into the cavernous sinus and/or the lower third of the clivus, extended transbasal approach is selected. Lesions that extend further laterally, outside of the boundaries formed by the carotid arteries at the foramen lacerum, are considered for either a lateral approach or a staged procedure.

ACKNOWLEDGMENTS

The authors thank Dr. Shouren Shih for preparation of cadaveric specimens and Ms. Jodi L. Brower for excellent medical illustrations.

REFERENCES

1. Frazier CH. An approach to the hypophysis through the anterior cranial fossa. Ann Surg 1913;57:145–150

2. Derome PJ. Transbasal approach to tumors invading the skull base. In: Schmidek HH, Sweet WH, eds. Operative Neurosurgical Techniques Indications, Methods, and Results. Philadelphia: W.B. Saunders Company 1993, 427–441
3. Tessier P, Guiot G, Derome P. Orbital hypertelorism. II. Definite treatment of orbital hypertelorism by craniofacial or by extracranial osteotomies. Scand J Reconstr Surg 1973;7:39–58
4. Sekhar LN, Nanda A, Sen CN, Snyderman CN, Janecka IP. The extended frontal approach to tumors of the anterior, middle, and posterior skull base. J Neurosurg 1992;76:198–206
5. Arita N, Mori S, Sano M, et al. Surgical treatment of tumors in the anterior skull base using the transbasal approach. Neurosurgery 1989;24:379–384
6. Jane JA, Park TS, Pobereskin LH, Winn HR, Butler AB. The supraorbital approach: Technical note. Neurosurgery 1982;11: 537–542
7. Johns ME, Kaplan MJ, Jane JA, Park TS, Cantrell RW. Supraorbital rim approach to the anterior skull base. Laryngoscope 1984;94:1137–1139
8. Kawakami K, Yamanouchi Y, Kawamura Y, Matsumura H. Operative approach to the frontal skull base: Extensive transbasal approach. Neurosurgery 1991;28:720–725
9. Kawakami K, Yamanouchi Y, Kubota C, Kawamura Y, Matsumura H. An extensive transbasal approach to frontal skull-base tumors. Technical note. J Neurosurg 1991;74:1011–1013
10. Raveh J, Turk JB, Ladrach K, et al. Extended anterior subcranial approach for skull base tumors: Long-term results. J Neurosurg 1995;82:1002–1010
11. Spetzler RF, Hermen JM, Beals S, Joganic E, Milligan J. Preservation of olfaction in anterior craniofacial approaches. J Neurosurgery 1993;79:48–52
12. Fijitsu K, Saijoh M, Aoki F, et al. Telecanthal approach for meningiomas in the ethmoid and sphenoid sinuses. Neurosurgery 1991;28:714–720
13. Fujii K, Chambers SM, Rhoton AL. Neurovascular relationship of the sphenoid sinus. A microsurgical study. J Neurosurg 1979;50:31–39
14. Ouaknine GE, Hardy J. Microsurgical anatomy of the pituitary gland and the sellar region. 2. The bony structure. Am Surg 1987;53:291–297
15. Kraus DH, Shah JP, Arbit E, Galicich JH, Strong EW. Complications of craniofacial resection for tumors involving the anterior skull base. Head Neck 1994;16:307–312